U. S. NAVAL ORDNANCE TEST STATION

W. W. Hollister, Capt., USN
Commander

Wm. B. McLean, Ph.D.
Technical Director

NOTS TP 2346 NAVORD REPORT 6606

BASE-VENTED HYDROFOILS

By

T. G. Lang

Research Department

Copy № 174

China Lake, California
19 October 1959

NOTS Technical Publication 2346
NAVORD Report 6606

Published by . . . . . Research Department
Manuscript 508/MS-2
Collation . . . . . Cover, 20 leaves, abstract cards
First printing . . . . . 200 numbered copies
Security classification . . . . . UNCLASSIFIED

FOREWORD

The Research and Underwater Ordnance Departments of the U. S. Naval Ordnance Test Station have been engaged in an experimental and theoretical investigation of vented hydrofoils. This report presents calculations to show the feasibility of base venting on lifting hydrofoils to improve cavitation resistance and efficiency. Further theory that extends the former cavity theory to the case of an arbitrary vented hydrofoil, operating at zero cavity number, will be published in NAVORD Report 7005 (Ref. 6).

Another report in process of publication, NAVORD Report 7008 (Ref. 5), will give results of water-tunnel tests on hydrofoils in which gas is exhausted through holes on the side. The main purpose of these tests was to show that large changes in lift occur as a result of gas venting. In torpedo and other underwater application, gas can be exhausted through holes in the stabilizing surfaces for control purposes, allowing the substitution of gas valves and lines for the usual linkages and control surfaces.

This work was supported by Foundational Research Task Assignment NO-000-283/32015/02060 and Bureau of Ordnance Task Assignment NO-404-664/41001/01060, in the period February through August 1959.

This report is transmitted for information only. It does not represent the official views or final judgment of the U. S. Naval Ordnance Test Station, and the Station assumes no responsibility for action taken on the basis of its contents.

RENÉ L. ENGEL
Head, Oceanic Research Division

Released under
the authority of:
WILLIAM S. McEWAN
Head, Research Department (Actg.)

ABSTRACT

Lift-producing hydrofoils that operate with a portion of the surface vented with gas have been analyzed. The gas-covered surface is defined as the base.

Results of the analysis show that a large number of different types of base-vented hydrofoils exist, some of which may have greater cavitation resistance and higher efficiency than the best of the fully wetted hydrofoils, provided, of course, that sufficient gas is available for venting.

Other results show that a cambered base-vented hydrofoil having a parabolic cross section can operate near the surface without vapor cavitation, at speeds as much as 50% greater than those of fully wetted hydrofoils, and with little sacrifice in efficiency.

Experimental tests on base-vented hydrofoils are needed to verify the results of this analysis.

CONTENTS

INTRODUCTION

Hydrofoils are used for such varied purposes as propeller blades, keels and rudders of surface craft, stabilizing fins and control surfaces of underwater bodies, and support struts and lifting surfaces of the so-called hydrofoil craft. These hydrofoils having streamlined cross sections and operating in a fully wetted condition are very efficient at speeds up to the beginning of cavitation. As cavitation increases, however, there is a corresponding increase in the number and degree of undesirable characteristics: pitting of the hydrofoil surface, noise, drag, reduction in lift, and unsteady performance. The critical speed at which cavitation begins for a given depth is a function of the hydrofoil geometry, and it increases (improves) as the thickness is reduced, as the angle of attack approaches the design angle, and as the sweepback increases.

Supercavitating hydrofoils have recently been developed by the Navy on the basis of research done at the David Taylor Model Basin (Ref. 1). The typical cross section of these hydrofoils is so designed that a cavity bubble springs from the thin, sharp leading edge and extends past the trailing edge without the upper surface ever contacting the water. The lower surface, usually concave, never cavitates because it is designed to operate at pressures greater than the static depth pressure. The shape of the upper surface does not matter so long as it does not come in contact with the cavity wall. This design provides steady and predictable lift and drag at high speeds, and it eliminates the pitting problem that results from the cavity collapsing on the hydrofoil. A modification of this design, sometimes called a superventilating hydrofoil, is obtained by venting gas into the cavity. The supercavitating type of hydrofoil has less efficiency and structural strength than the more common fully wetted streamlined hydrofoil; the latter type is generally used up to as high a noncavitating speed as possible.

This report introduces the concept of the base-vented hydrofoil, with characteristics midway between the fully wetted and the supercavitating types. It is still susceptible to cavitation, but the critical speed at which cavitation begins can be delayed appreciably. There is a large family of base-vented hydrofoils, many of which have high efficiency, high structural strength, and a wide range of operating angles of attack without cavitation.

DESCRIPTION

Base-vented hydrofoils (Fig. 1) are characterized by an upper and a lower surface, which may be unequal in length, joined at the leading edge and intersecting a third surface at their rear edges. This third surface is called the base. The leading edge can be either round or sharp, and is usually much thicker than that of supercavitating hydrofoils.

The base-vented hydrofoil operates with the upper and lower surfaces fully wetted and with the region behind the base vented with gas. The thick base permits the critical cavitation speed to be greatly increased and allows the lower surface to provide a larger portion of the lift when this is desirable. Venting of the region behind the base with gas reduces drag, which would be considerable if this base were fully wetted and if this region were filled with a highly turbulent wake. Gas will easily replace water when it is vented into a wake at some point along it or when the wake intersects an adequately large gas reservoir.

EFFICIENCY

The efficiency of any hydrofoil may be regarded as being its lift-to-drag ratio: for a given lift the efficiency is improved as the drag is reduced. The efficiency of a base-vented hydrofoil could be either greater or less than that of a fully wetted hydrofoil, depending on the shape and the pressure behind the base. The efficiency of a fully wetted hydrofoil is, for the NACA 16-series cross sections (Ref. 2),

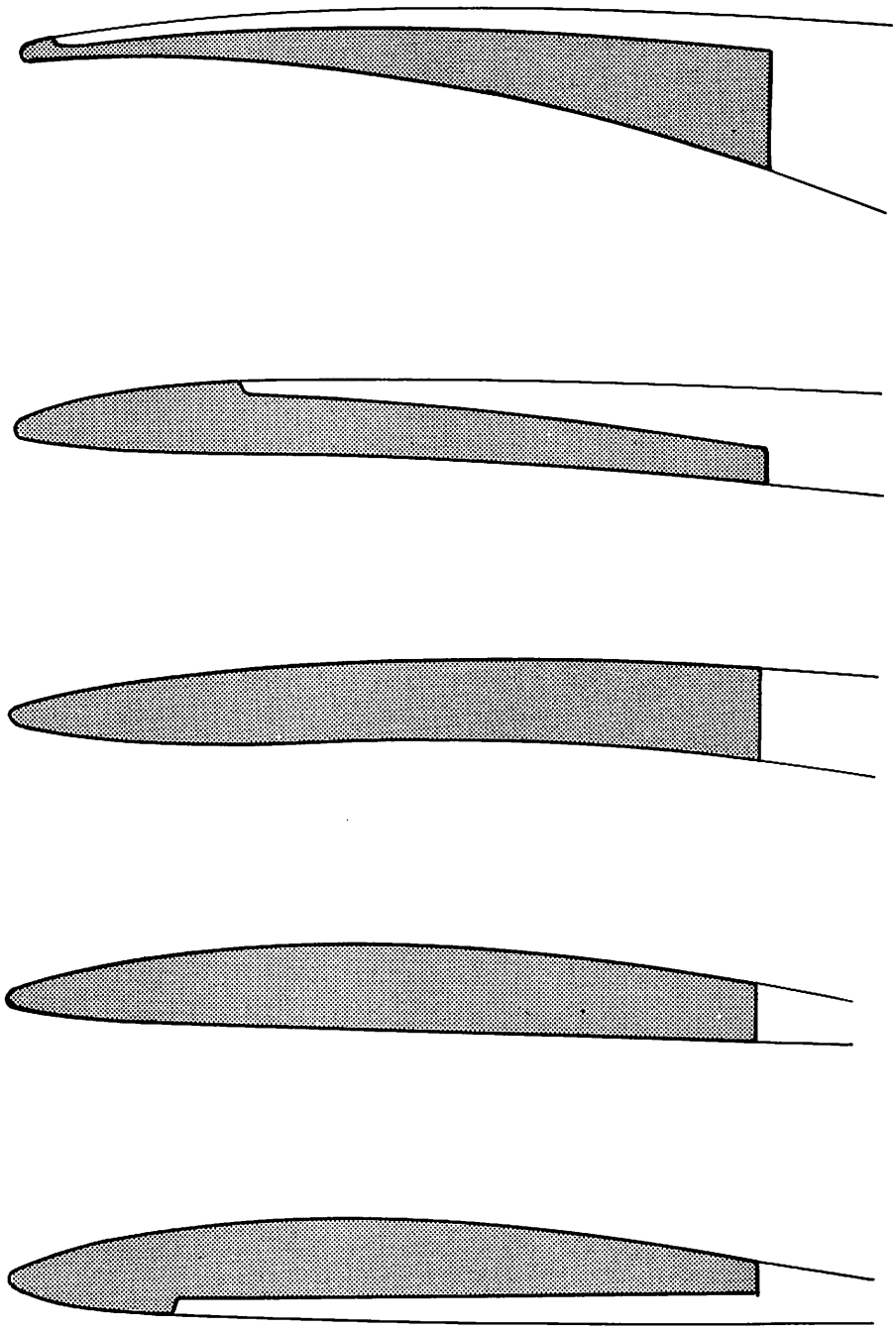

FIG. 1. A Typical Family of Base-Vented Hydrofoils.

$$(1) \qquad \frac{L}{D} = \frac{C_L}{C_D} = \frac{C_L}{2C_f \left(\frac{V_{av}}{V_o}\right)^2} \doteq \frac{C_L}{2C_f \left(1 + 2.3\frac{t_o}{c}\right)}$$

where

A = planform area, ft^2

c = chord length, ft

C_D = drag coefficient $\dfrac{D}{\frac{1}{2}\rho A V_o^2}$

C_f = skin-friction coefficient

C_L = lift coefficient $\dfrac{L}{\frac{1}{2}\rho A V_o^2}$

t_o = maximum thickness, ft

V_{av} = average root-mean-square velocity on the hydrofoil surface, ft/sec

V_o = free-stream velocity, ft/sec

The lift coefficient at zero angle of attack for a two-dimensional hydrofoil having a circular arc camber line is

$$C_{L_o} = 12.5\frac{f}{c}$$

where f is the maximum ordinate of the camber line.

From the viewpoint of cavitation resistance, a uniform pressure distribution along the chord is optimum, such as that theoretically produced by the NACA "a = 1.0" camber line (Ref. 2). However, experimentation shows that only about 75% of the theoretical lift is actually obtained, thereby indicating that the cavitation resistance is only 75% of optimum. The circular arc

camber line, however, theoretically produces an elliptical pressure distribution which, by definition, provides a cavitation resistance about 75% of optimum. Since, in this instance, theory (Ref. 2) is verified by experiment, it may be stated that the circular arc camber line provides about the same cavitation resistance as the "a = 1.0" camber line. Moreover, if the angle of attack deviates somewhat from zero during operation, the circular arc camber line is desirable because its elliptical pressure distribution permits a small lift increase without materially affecting its cavitation characteristics.

The efficiency of a base-vented hydrofoil whose upper and lower surfaces have equal lengths and equal but opposite pressure coefficients is

$$(2) \qquad \frac{L}{D} = \frac{C_L}{C_D} \doteq \frac{C_L}{2C_f \left(\frac{V_{av}}{V_o}\right)^2 + C_{D_c}} \doteq \frac{C_L}{2C_f + C_{D_c}}$$

The term C_{D_c} is the cavity drag coefficient and is shown in Ref. 3 for uncambered struts to be

$$(3) \qquad C_{D_c} = C_{D_o}\left[1 + K + 0(K^2)\right] = \frac{\text{cavity drag}}{bc \cdot \frac{1}{2}\rho V_o^2}$$

where

$$(4) \qquad K = \frac{P_o - P_c}{\frac{1}{2}\rho V_o^2} = \text{ventilation number of the gas cavity}$$

and where

b = hydrofoil span, ft

P_o = free-stream static pressure, lb/ft^2

P_c = pressure in the cavity, lb/ft^2

If $K << 1.0$, $C_{D_c} \doteq C_{D_o}$ where C_{D_o} is the cavity drag coefficient when $K = 0$.

The following expression for C_{D_o} is derived in Ref. 3 for base-vented uncambered struts:

$$C_{D_o} = \frac{2}{\pi c} \left(\int_o^c \frac{dy}{dx} \cdot \frac{dx}{\sqrt{c - x}} \right)^2 \tag{5}$$

The values of C_{D_o} for various base-vented strut cross sections are

0.0 for the low-drag cross sections (to be discussed later)

0.28 $(t_o/c)^2$ for the circular arc (surfaces parallel at trailing edge)

0.39 $(t_o/c)^2$ for the parabola

0.64 $(t_o/c)^2$ for the wedge

where

x = distance from the leading edge, ft

y = semithickness of strut at station x, ft

In order to calculate the lift and drag coefficients of base-vented hydrofoils whose surfaces are equal, it is assumed here that the drag for a near-zero angle of attack is equal to the drag of the uncambered cross section, and that the lift is equal to the theoretical lift of the camber line. Reasoning from the physical viewpoint, it may be argued that the cavity drag should be independent of camber and small angles of attack, since the boundary conditions of cavity pressure and the relative slopes of the walls of the cavity and the thickness of the cavity at its forward end where it joins the hydrofoil base remain constant. This assumption is believed to be further justified on the basis of the similarity between base-vented hydrofoils and fully wetted hydrofoils and the fact that Ref. 2 shows that the pressure coefficients of camber and thickness are additive for thin fully wetted hydrofoils

having low to moderate camber. The boundary conditions are similar for both types of hydrofoils, since in each case the flow must leave the trailing edge tangentially and the pressure immediately behind the trailing edge or base must remain unaffected by camber.

CAVITATION

In most applications of hydrofoils, it is necessary to estimate the cavitation resistance. Both fully wetted and base-vented hydrofoils will cavitate when the operating cavitation number σ equals the incipient cavitation number σ_i. The incipient cavitation number of a hydrofoil is defined as being approximately equal to the negative value of the minimum pressure coefficient $(C_p)_{min}$ on the hydrofoil, or

$$\sigma_i \doteq -(C_p)_{min} = \frac{P_o - P_{min}}{\frac{1}{2}\rho V_o^2} = \left(\frac{V_{max}}{V_o}\right)^2 - 1 \tag{6}$$

where

P_{min} = minimum static pressure on the surface of the hydrofoil, lb/ft^2

V_{max} = maximum velocity on the surface of the hydrofoil, fps

The operating cavitation number σ is defined as

$$\sigma = \frac{P_o - P_v}{\frac{1}{2}\rho V_o^2}$$

If the water is below 100°F, the vapor pressure P_v will be close to zero. Consequently,

$$\sigma \doteq \frac{P_o}{\frac{1}{2}\rho V_o^2}$$

Consider, for example, a two-dimensional uncambered parabola. It is known that the pressure P on each surface of a parabola is everywhere greater than or equal to P_o; hence, the incipient cavitation number is zero at zero angle of attack. Therefore a parabola cannot cavitate at any speed when the angle of attack is zero.

The incipient cavitation number of a fully wetted hydrofoil is now considered. For the near-optimum NACA 16-series of fully wetted hydrofoils having a circular arc camber line (Ref. 2)

$$\sigma_i \doteq \left(1 + 1.15 \frac{t}{c} + 0.32\, C_L\right)^2 - 1$$

When $t/c << 1.0$ and $0.32\, C_L << 1.0$, σ_i can be simplified to

$$\sigma_i \doteq 2.3 \frac{t}{c} + 0.64\, C_L \tag{7}$$

The incipient cavitation number of base-vented hydrofoils cannot be expressed so simply because of the wide variety of possible shapes. For the specific case of a hydrofoil having a parabolic thickness distribution and a circular arc camber line,

$$\sigma_i = 0.64\, C_L \tag{8}$$

The incipient cavitation number σ_i of a base-vented hydrofoil can be greater than $0.64\, C_L$ or it can be zero. It may be zero when all the lift is developed from positive pressures acting on the lower surface while the upper surface follows the free-stream line $P = P_o$. Since the upper surface contributes no lift, it might as well be vented from its leading edge to reduce the frictional drag. This limiting case of a base-vented hydrofoil approaches, by definition, a superventilating hydrofoil. In Ref. 4 it is shown that the maximum L/D of this type of hydrofoil is 17 if the pressures on the lower surface are always to be positive and if the upper surface is to lie within the free-stream line $P = P_o$.

The other extreme of a base-vented hydrofoil is one in which all the lift is developed from negative pressures (relative to the

free-stream static pressure) acting on the upper surface while the lower surface follows the free-stream line $P = P_o$. In this case, for uniform chordwise loading, the incipient cavitation number will be equal to the lift coefficient. The lower surface can be vented from the leading edge to reduce frictional drag. This type of hydrofoil is discussed more thoroughly later in this report.

BASE-VENTED HYDROFOIL WITH ZERO CAVITY DRAG

In vented flow, the pressure on a hydrofoil may be less than the pressure in the gas cavity without the gas cavity springing forward (Ref. 5). Consequently it is possible to reduce the cavity drag to zero if $K = 0$, when (Eq. 5)

$$C_{D_o} = \frac{2}{\pi c}\left(\int_o^c \frac{dy}{dx}\cdot\frac{dx}{\sqrt{c-x}}\right)^2 = 0$$

An uncambered biconvex circular arc strut cut off at some point $x = c$ might first be considered. Then the upper ordinate, measured from the center line at a distance x from the leading edge and linearized by assuming a thin profile, is found to be

$$y = 2t_o\left(\frac{x}{c_o} - \frac{x^2}{c_o^2}\right) \tag{9}$$

where c_o = chord length of the biconvex strut with no cutoff, and t_o = maximum thickness of the biconvex circular arc strut. Now, after differentiating to obtain dy/dx, substituting in Eq. 5, integrating, and simplifying, the cavity drag coefficient is found to be

$$C_{D_o} = \frac{32}{\pi}\left(\frac{t_o}{c_o}\right)^2\left(1 - \frac{4}{3}\frac{c}{c_o}\right)^2 = \frac{\text{cavity drag per unit span}}{\frac{1}{2}\rho c V_o^2} \tag{10}$$

Hence, for $C_{D_o} = 0$, $c = 3/4\ c_o$ and $t = 3/4\ t_o$.

A second interesting example of a base-vented hydrofoil having zero cavity drag is the modified parabola whose thickness distribution is described by the ordinate of the upper surface

(11) $$y = C_1 \sqrt{X} - C_2 X^2$$

where

$$\frac{dy}{dx} = \frac{C_1}{2\sqrt{X}} - 2C_2 X$$

The arbitrary constants C_1 and C_2 are evaluated in terms of the base thickness t and chord c; then Eq. 5 is integrated and the cavity drag is seen to be zero when

$$c = 1.77\ c_{(t = t_o)}$$

$$t = 0.73\ t_o = \text{thickness at the base}$$

$$y = 0.525\ t_o \left[1.70 \sqrt{\frac{x}{c}} - \left(\frac{x}{c} \right)^2 \right]$$

where t_o = maximum thickness.

A third example of a cross section having zero cavity drag and good cavitation resistance is a modified 16-series hydrofoil cut off at the appropriate chord length for which the cavity drag is zero. This 16-series cross section can be matched closely by the equation for the modified parabola presented above. It is not necessary to perform the integration to obtain $C_{D_o} = 0$, since this section is so close to the modified parabola and since the criterion for zero cavity drag appears to be satisfied when the ratio of the base thickness to maximum thickness t_o is about 0.73 to 0.75 as shown by the examples of the modified parabola and the circular arc. Therefore, if the 16-series hydrofoils are cut off where $t = 0.73\ t_o$, the cavity drag will be approximately zero. The chord length c will be 0.78 times the fully wetted chord length c_o. The thickness distribution of this hydrofoil is shown in Fig. 2.

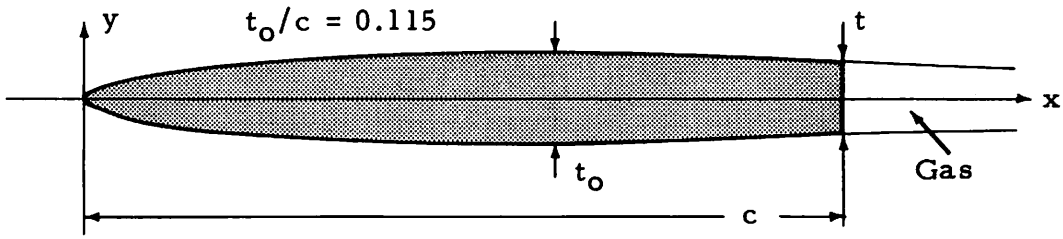

$\frac{x}{c}$	$\frac{t_x}{t_o}$
000.00	000.00
001.60	021.53
003.21	030.09
006.41	041.82
009.62	050.53
010.82	057.62
019.23	068.91
025.64	077.73
038.46	090.29
051.28	097.58
064.10	100.00
076.92	097.24
089.74	087.82
100.00	073.00

FIG. 2. Thickness Distribution of Base-Vented Cut-Off 16-Series Hydrofoil With Zero Cavity Drag.

The static pressure will be increased from that of the basic 16-series to cavity pressure near the cutoff; therefore, the incipient cavitation number will be slightly less than that of a fully-wetted 16-series hydrofoil having the same thickness. Based on the cut-off chord length c, the incipient cavitation number of the modified cut-off 16-series hydrofoil with a circular arc camber line is (from Ref. 2)

$$\sigma_i \doteq \left[1 + 1.10 \left(\frac{t_o}{c} \right) (0.78) + 0.32\, C_L \right]^2 - 1$$

If it is assumed that $1.10 \left(\frac{t_o}{c} \right) (0.78) << 1.0$ and $0.32\, C_L << 1.0$, then

$$\sigma_i \doteq 1.74 \frac{t_o}{c} + 0.64\, C_L \tag{13}$$

The L/D ratio of this hydrofoil at zero angle of attack is

$$\frac{L}{D} = \frac{C_L}{C_D} = \frac{C_L}{2C_f\left(1 - C_{P_{av}}\right)} \doteq \frac{C_L}{2C_f\left(1 + 1.5\,\frac{t_o}{c}\right)} \tag{14}$$

In performing these calculations to obtain base-vented sections having zero cavity drag, it is assumed that the boundary conditions in the linearized theory used in Ref. 3 for deriving Eq. 5 are physically realistic. The validity of this assumption has been partially verified by the experiments of Ref. 5.

BASE-VENTED HYDROFOIL WITH OPTIMUM EFFICIENCY

If it is assumed that a base-vented hydrofoil has a thickness distribution that produces zero cavity drag for K = 0 and has an elliptical pressure distribution, it can then be cambered by using a circular-arc camber line such that the net static pressure on the lower surface is P_o. The static pressure on the upper surface will still be elliptical. Since the pressure everywhere on the lower surface is P_o, this surface can be vented shortly behind the leading edge on the lower surface in order to reduce the frictional drag. At zero angle of attack, neither the lift nor the upper-surface pressure distribution will be affected.

For this example,

$$\sigma_i = 1.28\, C_L \tag{15}$$

$$\frac{L}{D} = \frac{C_L}{C_D} = \frac{C_L}{C_f\left(\frac{V_{upper}}{V_o}\right)^2_{av}} \doteq \frac{C_L}{C_f(1 + C_L)} \tag{16}$$

The table below shows efficiency and incipient cavitation number of this section as a function of design lift coefficient. The assumptions made for this tabulation are K = 0, α = 0, $AR = \infty$, C_f = 0.0039, a circular arc camber line, and no flow separation on the wetted surface. It should be noted that the cavitation resistance is not quite optimized because of the use of an elliptical upper-surface pressure distribution. However, this elliptical pressure distribution permits the angle of attack to vary slightly without materially increasing the incipient cavitation number.

C_L	L/D	σ_i
1.0	128	1.28
0.8	114	1.02
0.6	96	0.77
0.5	86	0.64
0.4	73	0.51
0.3	59	0.38
0.2	42	0.26
0.1	23	0.13

The cross section of this hydrofoil can be approximated by superposing an NACA 66-series hydrofoil that is cut off at t = 0.73 t_o and a circular arc camber line whose minimum pressure equals the minimum pressure of the modified 66-series hydrofoil. This minimum pressure as a function of the cut-off chord length c is $-1.8\, t_o/c$. The minimum pressure produced by a circular arc meanline is $-0.64\, C_L$. Therefore

$$-1.8 \frac{t_o}{c} = -0.64\, C_L$$

or

$$C_L = 2.81 \frac{t_o}{c} \tag{17}$$

The offsets of this section and a typical cross section having $C_L = 0.5$ are shown in Fig. 3. It should be noted that the lower surface in the region behind the venting point should lie within the lower surface streamline shown in Fig. 3. This lower surface may be vented by exhausting gas through chordwise slits or holes or by exhausting gas into the region behind a discontinuity as shown by the dotted lines of Fig. 3.

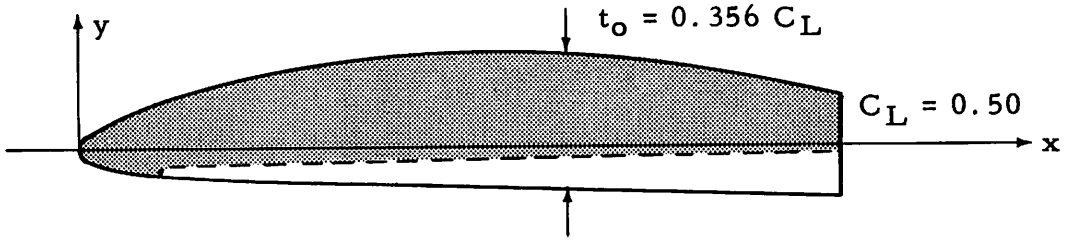

$\frac{x}{c}$	$\frac{y_{upper}}{cC_L}$	$\frac{y_{lower}}{cC_L}$
0.0000	0.0000	0.0000
0.0070	0.0292	0.0248
0.0106	0.0358	0.0291
0.0176	0.0461	0.0351
0.0352	0.0648	0.0431
0.0704	0.0952	0.0533
0.1056	0.1205	0.0600
0.1409	0.1425	0.0651
0.2113	0.1789	0.0723
0.2817	0.2071	0.0776
0.3521	0.2282	0.0822
0.4226	0.2430	0.0869
0.4930	0.2504	0.0935
0.5634	0.2549	0.0975
0.6338	0.2522	0.1036
0.7042	0.2435	0.1102
0.7747	0.2290	0.1173
0.8451	0.2079	0.1241
0.9155	0.1778	0.1283
0.9860	0.1392	0.1303
1.0000	0.1299	0.1299

FIG. 3. Coordinates of a Base-Vented Hydrofoil With Optimum Efficiency and Near-Optimum Cavitation Resistance.

APPLICATION OF BASE-VENTED HYDROFOILS

In designing a base-vented hydrofoil for a practical application, it is important to obtain the desired amount of venting, to keep K near zero, and to make sufficiently accurate estimates of the efficiency, incipient cavitation, and strength of the section.

Tests were conducted on hydrofoil models with air forced through holes in their surfaces (Ref. 5). Results showed that the air never sprang forward on the surface ahead of the exhaust holes unless the water ahead of this point had already separated as a result of the hydrofoil's stalling or cavitating. The tests also showed that the cavitation number of the air cavity could not be reduced below 0.05. This is believed to have been caused by tunnel-wall interference, since the recorded values of K were in agreement with tunnel blockage theory.

These tests also showed that a minimum air-flow rate Q_{min} is required to form an air cavity that would extend past the trailing edge of the hydrofoil. Although this value may be a function of the water-tunnel dimensions, it was found to be

$$Q_{min} \doteq 0.07\, t'bV_o \tag{18}$$

where t'b is the projected area in the streamwise direction of the surface of the hydrofoil covered by air. It is believed that, without tunnel-wall interferences, a base-vented hydrofoil can be adequately vented so that K approaches zero.

If a hydrofoil at a depth z were vented with air from the surface, and if the air were to move unrestricted down from the surface to the hydrofoil, the ventilation number K would be

$$K = \frac{\rho g z}{\frac{1}{2}\rho V_o^2} \tag{19}$$

At high speeds and shallow depths, $K \doteq 0$.

Another interesting feature of base-vented hydrofoils is that as their efficiency is improved, their cavitation resistance is reduced. The base-vented hydrofoil whose upper surface is vented represents the one extreme of infinitely high cavitation resistance with low to moderate efficiency, and the hydrofoil whose lower surface is vented represents a section having only moderate cavitation resistance but high efficiency. The base-vented cambered parabola has intermediate characteristics.

In some applications where strength and susceptibility to damage are controlling factors, the base-vented hydrofoil may be highly desirable because its base is thick compared to the fully wetted hydrofoil's thin, sharp trailing edge. Also, because of its blunt base, it is possible to design the base-vented hydrofoil for a more extensive region of laminar flow than can be obtained on an equivalent fully wetted hydrofoil.

Tests were conducted on a base-vented parabola cambered to $C_L = 0.4$, using the NACA "a = 1.0" camber line (Fig. 4). The results of these tests will be published in a future report. It is planned to conduct further tests on base-vented hydrofoils with zero cavity drag. Data will be obtained on the effect of air-flow rate on the ventilation number of the gas cavity.

COMPARISON OF FULLY WETTED AND BASE-VENTED HYDROFOILS

A number of different comparisons can be made of fully wetted and base-vented hydrofoils. The superiority of one type over the other depends on the specific application. In general, the best hydrofoil will be the one that has the greatest efficiency or L/D ratio and, at the same time, that satisfies the strength and cavitation requirements. Sometimes an increase in thickness is desirable, for example to prevent cavitation when there is a large variation in the operating angles of attack. In another application, where the hydrofoil pierces a water - gas interface, an important design consideration would be susceptibility to sporadic gas venting.

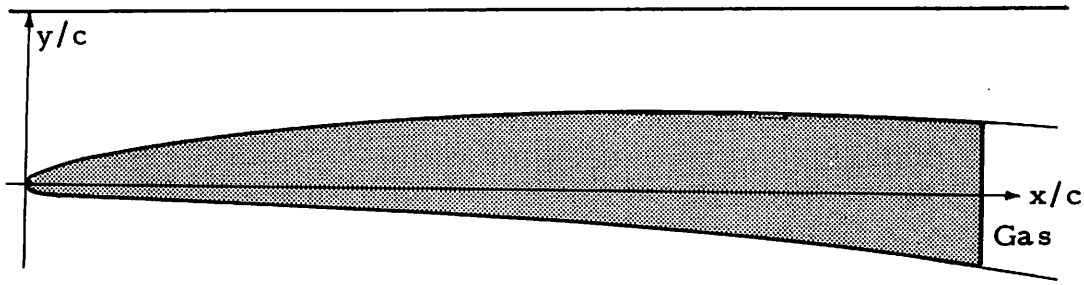

$\frac{x}{c}$	$\frac{y_{upper}}{c}$	$\frac{y_{lower}}{c}$
0.0000	0.00000	0.00000
0.0050	0.00630	0.00430
0.0075	0.00790	0.00510
0.0125	0.01053	0.00625
0.0250	0.01558	0.00814
0.0500	0.02308	0.01046
0.0750	0.02902	0.01206
0.1000	0.03403	0.01337
0.1500	0.04252	0.01558
0.2000	0.04947	0.01763
0.2500	0.05540	0.01960
0.3000	0.06048	0.02162
0.3500	0.06490	0.02370
0.4000	0.06887	0.02603
0.4500	0.07220	0.02840
0.5000	0.07506	0.03094
0.5500	0.07750	0.03370
0.6000	0.07947	0.03663
0.6500	0.08110	0.03990
0.7000	0.08218	0.04332
0.7500	0.08285	0.04705
0.8000	0.08302	0.05118
0.8500	0.08262	0.05568
0.9000	0.08153	0.06087
0.9500	0.07941	0.06679
1.0000	0.07500	0.07500

FIG. 4. Coordinates of a Cambered Base-Vented Parabola. C_{L_O} = 0.4, "a = 1.0" camber line, t/c = 0.15.

Two comparisons between the two types will be made. For the first comparison, it will be assumed that a hydrofoil must have a given lift coefficient and a given thickness-to-chord ratio. A base-vented hydrofoil having a parabolic thickness distribution will be used in the first comparison. The critical speed at which cavitation begins is considered to be the most important characteristic. It should be remembered that although the efficiency of a base-vented hydrofoil may be increased, it will be done at the expense of a reduced critical cavitation speed, and vice versa. Therefore, the parabolic cross section represents only one specific type of base-vented hydrofoil and is not necessarily optimum. On the other hand, the NACA 16-series hydrofoil on the basis of both efficiency and cavitation represents a near-optimum fully wetted hydrofoil. From Table 1 it can be seen that the cambered parabola may be used near the water surface without cavitating at speeds as much as 30 knots greater than the speed of a fully wetted hydrofoil. The efficiency is lower, but still comparable.

In the second comparison, shown in Table 2 and Fig. 5, both the lift and strength are held constant and the cavitation number is varied. As the operating cavitation number is reduced, the hydrofoils will tend to cavitate. At this point, the chord length is increased to prevent cavitation, and the thickness is modified in such a way that the lift and strength of the hydrofoil remain constant. This comparison is probably more typical of an actual application than the first one.

The bending stress f on a hydrofoil caused by a moment M is

$$f = \frac{M}{jct^2} \propto \frac{Lb}{jct^2}$$

where

b = span, ft
j = strength factor and a function of cross-sectional shape
j_1 = 0.091 for the fully wetted NACA 16-series (Hydrofoil A)
j_2 = 0.067 for the base-vented parabola (Hydrofoil B)
j_3 = 0.112 for the base-vented modified parabola or cut-off NACA 16-series (Hydrofoil C)
L = lift

TABLE 1. Comparison of Hydrofoils With Equal Lift Coefficients and Thickness-to-Chord Ratios

Assumptions:

1. Turbulent flow
2. Re = 2×10^6, Cf = 0.0039
3. Equal C_L and t/c
4. Circular arc camber line
5. K ≐ 0
6. $\alpha = 0°$
7. $AR = \infty$
8. No sweepback

Hydrofoil Type[a]	C_L	t/c	C_D	L/D	σ_i	V_{cr} at Water Surface, Knots
A	0.50	0.15	0.0101	49	0.67	33
B			0.0166	30	0.32	48
A	0.25	0.15	0.0101	25	0.51	38
B			0.0166	15	0.16	68
A	0.50	0.10	0.0094	53	0.55	37
B			0.0117	43	0.32	48
A	0.25	0.10	0.0094	27	0.39	43
B			0.0117	21	0.16	68
A	0.50	0.05	0.0086	58	0.44	41
B			0.0088	57	0.32	48
A	0.25	0.05	0.0086	29	0.28	51
B			0.0088	28	0.16	68

[a] A = fully wetted NACA 16-series.
B = base-vented cambered parabola.

TABLE 2. Comparison of Hydrofoils With Equal Lift and Strength

Assumptions:

1. Turbulent flow
2. $Re = 2 \times 10^6$, $C_f = 0.0039$
3. Circular arc camber line
4. $\alpha = 0°$
5. $K = 0$
6. V_o = constant
7. Strength = strength of fully wetted 16-series where $t/c = 0.10$, $c = c_o$, $C_L = 0.50$
8. $AR = \infty$
9. No sweepback

Hydrofoil Type[a]	σ	c/c_o	t/c	C_L	C_D	L/D
A	≥ 0.55	1.00	0.100	0.50	0.0094	53
B		1.00	0.117	0.50	0.0132	38
C		1.00	0.090	0.50	0.0089	56
A	0.50	1.09	0.088	0.46	0.0092	50
B		1.00	0.117	0.50	0.0132	38
C		1.00	0.090	0.50	0.0089	56
A	0.40	1.25	0.063	0.40	0.0087	46
B		1.00	0.117	0.50	0.0132	38
C		1.16	0.071	0.43	0.0086	50
A	0.30	1.67	0.047	0.30	0.0085	35
B		1.06	0.109	0.47	0.0124	38
C		1.47	0.049	0.34	0.0084	40
A	0.20	2.38	0.027	0.21	0.0082	26
B		1.61	0.058	0.31	0.0091	34
C		2.20	0.028	0.23	0.0081	28
A	0.10	4.50	0.011	0.11	0.0080	14
B		3.10	0.020	0.16	0.0080	20
C		3.85	0.012	0.13	0.0079	17

[a] A = fully wetted NACA 16-series.
B = Base-vented cambered parabola.
C = Base-vented cut-off NACA 16-series.

$$\sigma_{i(\text{Hydrofoil C})} = 1.74\, t_o/c + 0.64\, C_L$$

$$= 0.44\, C_L^{3/2} + 0.64\, C_L$$

The thickness-to-chord ratios are

$$(t/c)_{\text{Hydrofoil A}} = 0.282\, C_L^{3/2}$$

$$(t/c)_{\text{Hydrofoil B}} = 0.329\, C_L^{3/2}$$

$$(t_o/c)_{\text{Hydrofoil C}} = 0.253\, C_L^{3/2}$$

The C_L/C_D ratios where $C_f = 0.0039$ for turbulent flow at a Reynolds number $Re = 2 \times 10^6$ are

$$(C_L/C_D)_{\text{Hydrofoil A}} = \frac{C_L}{2C_f\,(1 + 2\,t/c)} = \frac{C_L}{0.0078\,(1 + 2\,t/c)}$$

$$(C_L/C_D)_{\text{Hydrofoil B}} = \frac{C_L}{2C_f + 0.39\,(t/c)^2} = \frac{C_L}{0.0078 + 0.39\,(t/c)^2}$$

$$(C_L/C_D)_{\text{Hydrofoil C}} = \frac{C_L}{2C_f\,(1 + 1.5\,t/c)} = \frac{C_L}{0.0078\,(1 + 1.5\,t/c)}$$

From Table 2 and Fig. 5, it is seen that the base-vented hydrofoils in this particular comparison have higher efficiency than the fully wetted hydrofoil over the full range of operational cavitation numbers. It must be emphasized, however, that a value of $K \doteq 0$ was assumed and may not be met in practice. It is also interesting to note that the cambered parabola in every instance has a greater thickness-to-chord ratio than the other hydrofoils and it becomes double that of the others at low values of σ.

For design purposes, a margin of safety of at least 50% should be used to include the effects of angle-of-attack changes,

manufacturing and alignment tolerances, etc. If efficiencies are calculated, using a value of $\sigma_{design} = 1.5\sigma$ and the assumptions of Table 2, and further assuming that operation is at the surface, it will be seen that the base-vented cut-off 16-series hydrofoil is most efficient up to a speed of 42 knots, the base-vented cambered parabola from 42 to 78 knots, and the superventilated hydrofoil above 78 knots. The cambered parabola is superior to the 16-series fully wetted hydrofoil at speeds above 40 knots.

The performance of the base-vented hydrofoil of optimum efficiency is indicated by the dotted line in Fig. 5. It is not listed in Table 2 because it cannot meet both the strength and lift requirements below $\sigma = 0.32$ owing to the added requirement that $t_o/c \leqq 0.355\ C_L$. It does meet these requirements above $\sigma = 0.32$, however, and when $C_L = 0.50$, the L/D ratio is 86, which is considerably higher than the fully wetted L/D ratio.

It can therefore be seen that base-vented hydrofoils may be highly desirable for use as propeller blades and the lifting surfaces of hydrofoil craft. Depending upon the operating conditions, any one of the family of base-vented hydrofoils (Fig. 1) can be used.

Further theory has subsequently been published in Ref. 6, which extends former cavity theory to the case of an arbitrary vented hydrofoil operating at zero ventilation number.

CONCLUSIONS

In summary, it can be stated that base-vented hydrofoils may have both significantly greater cavitation resistance and efficiency than fully wetted hydrofoils if the cavitation number of the gas cavity is near zero.

There is a complete family of base-vented hydrofoils that range from a hydrofoil having infinite cavitation resistance and low to moderate efficiency to a hydrofoil having moderate cavitation resistance with high efficiency. The cambered parabola represents a cross section having intermediate characteristics.

The drag of a base-vented hydrofoil is usually increased if the ventilation number is not near zero. Therefore, the effect of gas supply rate on the ventilation number should be more thoroughly investigated.

Additional tests on base-vented hydrofoils are planned. If the results of these tests verify the theory, base-vented hydrofoils may be advantageously used as the blades of propellers, pumps, and turbines, and as the lifting surfaces of hydrofoil craft.

NOMENCLATURE

A Planform area of hydrofoil, ft^2

AR Aspect ratio of hydrofoil

b Span of hydrofoil, ft

c Chord length of hydrofoil, ft

c_o Reference chord length of hydrofoil used in a specific analysis

C_1, C_2 Arbitrary constants

C_D Drag coefficient $= \dfrac{D}{\frac{1}{2}\rho A V_o^2}$

C_{D_c} Cavity drag coefficient $= \dfrac{\text{cavity drag}}{\frac{1}{2}\rho A V_o^2}$

C_{D_o} Cavity drag coefficient when K = 0

C_f Skin-friction coefficient $= \dfrac{\text{skin-friction drag}}{\frac{1}{2}\rho A V_o^2}$

C_L Lift coefficient $= \dfrac{L}{\frac{1}{2}\rho A V_o^2}$

C_{L_o} Design lift coefficient at zero angle of attack

C_p Pressure coefficient = $\dfrac{P - P_o}{\frac{1}{2}\rho V_o^2}$

D Drag of hydrofoil, lb

D' Drag coefficient based on base area = $\dfrac{D}{\frac{1}{2}\rho b t V_o^2}$

D_o' Drag coefficient based on base area when $K = 0$

f Bending stress, lb/in^2

g Acceleration of gravity = 32.2 ft/sec^2

j Strength factor for hydrofoil cross section

$j_{1, 2, 3}$ Strength factor for specific types of hydrofoils

K Cavitation number of gas cavity = $\dfrac{P_o - P_c}{\frac{1}{2}\rho V_o^2}$

k_1 Constant = jct^2, ft^3

k_2 Constant = $C_L c$, ft

L Lift of hydrofoil, lb

M Bending moment, ft-lb

P_c Cavity pressure, lb/ft^2

P_{min} Minimum pressure on the surface of the hydrofoil, lb/ft^2

P_o Free-stream static pressure, lb/ft^2

P_v Vapor pressure of water, lb/ft^2

Q_{min} Minimum air-flow rate required to fully ventilate a hydrofoil, ft^3/sec

Re Reynolds number = $\frac{V_o c}{\nu}$

t Thickness at the base of a hydrofoil whose surface lengths are equal, ft

t' Thickness of the gas-covered surface of a hydrofoil projected in the streamwise direction, ft

t_x Thickness at any point x, ft

V_{av} Average velocity over the surface of a hydrofoil, ft/sec

V_{cr} Velocity at which vapor cavitation begins, ft/sec at a specified depth

V_{max} Maximum velocity on the surface of a hydrofoil, ft/sec

V_o Free-stream velocity, ft/sec

x Coordinate of a hydrofoil measured rearward from the leading edge, ft

y Coordinate to the surface measured perpendicular from a line joining the center of the leading edge and the center of the base, ft

z Depth of the hydrofoil cross section below the water surface, ft

α Angle of attack, deg

ρ Density of water $\doteq$ 2 $slugs/ft^3$ for sea water

σ Operating cavitation number = $\frac{P_o - P_v}{\frac{1}{2}\rho V_o^2}$

σ_i Incipient cavitation number = $\dfrac{P_o - P_{min}}{\frac{1}{2}\rho V_o^2}$

ν Kinematic viscosity of water $\doteq 1.3 \times 10^{-5}$, ft^2/sec

REFERENCES

1. David Taylor Model Basin. Linearized Theory for Flows About Lifting Hydrofoils at Zero Cavitation Numbers, by M. P. Tulin and M. Burkhart. Carderock, Md., DTMB, February 1955. (DTMB C-638.)

2. National Advisory Committee for Aeronautics. Summary of Airfoil Data, by I. H. Abbott, A. E. von Doenhoff, and L. S. Stivers. Washington, NACA, 1945. (NACA Report 824.)

3. David Taylor Model Basin. Steady Two-Dimensional Cavity Flows About Slender Bodies, by M. P. Tulin. Carderock, Md., DTMB, May 1953. (DTMB Report 834.)

4. ------. Optimum Supercavitating Sections, by W. B. Morgan. Carderock, Md., August 1957. (DTMB C-856.)

5. U. S. Naval Ordnance Test Station. Water-Tunnel Tests of Side-Vented Hydrofoils, by T. G. Lang, D. A. Daybell, and K. E. Smith. China Lake, Calif., NOTS, 10 November 1959. (NAVORD Report 7008, NOTS TP 2363.) (In preparation.)

6. ------. Theoretical Lift and Drag on Vented Hydrofoils for Zero Cavity Number and Steady Two-Dimensional Flow, by Andrew G. Fabula. China Lake, Calif., NOTS, 4 November 1959. (NAVORD Report 7005, NOTS TP 2360.) (In preparation.)

INITIAL DISTRIBUTION

7 Chief, Bureau of Naval Weapons
- Ad3 (1)
- Req (1)
- ReO (1)
- ReO3 (1)
- ReU (1)
- ReU1 (1)
- ReU1-c (1)

2 Chief, Bureau of Aeronautics
- Code AD-3 (1)
- Code RS (1)

7 Chief, Bureau of Ships
- Code 106 (1)
- Code 312 (1)
- Code 370 (1)
- Code 421 (2)
- Code 442 (1)
- Code 560 (1)

1 Chief of Naval Operations

3 Chief of Naval Research
- Code 429 (1)
- Code 438 (1)
- Code 466 (1)

7 David W. Taylor Model Basin
- Code 142 (1)
- Code 500 (1)
- Code 513 (1)
- Code 523B (1)
- Code 580 (1)
- Code 800 (1)

1 Naval Aircraft Torpedo Unit, Naval Air Station, Quonset Point

1 Naval Air Development Center, Johnsville

1 Naval Engineering Experiment Station, Annapolis

2 Naval Ordnance Laboratory, White Oak
- Desk HL, Library Division (1)

1 Naval Postgraduate School, Monterey (Library, Technical Reports Section)

1 Naval Research Laboratory

1 Naval Torpedo Station, Keyport (Quality Evaluation Laboratory, Technical Library)

1 Naval Underwater Ordnance Station, Newport

3 Naval Weapons Plant (Code 752)
1 Navy Central Torpedo Office, Newport
1 Navy Electronics Laboratory, San Diego
1 Navy Mine Defense Laboratory, Panama City
1 Navy Underwater Sound Laboratory, Fort Trumbull
10 Armed Services Technical Information Agency (TIPCR)
1 Director of Defense (R&E) (Office of Fuels, Materials, and Ordnance, Bayard Belyea)
1 Langley Research Center (John Parkinson)
1 Maritime Administration (Coordinator for Research)
6 National Aeronautics & Space Administration
1 National Bureau of Standards (Fluid Mechanics Section, Dr. G. Schubauer)
1 Office of Technical Services
1 Aerojet-General Corporation, Azusa, Calif. (C. A. Gongwer) via InsOrd
1 Alden Hydraulic Laboratory, Worcester Institute, Worcester, Mass.
1 Applied Physics Laboratory, University of Washington, Seattle
1 Baker Manufacturing Company, Evansville, Wisc.
1 Bell Telephone Laboratories, Murray Hill, N. J.
1 Bendix Aviation Corporation, Pacific Division, North Hollywood
1 Bulova Research and Development Laboratories, Inc., Woodside, N. Y.
3 California Institute of Technology, Pasadena (Engineering Division)
Dr. A. J. Acosta (1)
Dr. M. S. Plesset (1)
Dr. T. Y. Wu (1)
1 Cleveland Pneumatics Industries, Inc., El Segundo, Calif. (Advanced Systems Development Division)
1 Clevite Research Center, Cleveland
1 CONVAIR Hydrodynamics Laboratory, San Diego
1 CONVAIR Scientific Research Laboratory, San Diego (A. L. Berlad)
1 Cornell University, Graduate School of Aeronautical Engineering, Buffalo (Prof. W. R. Sears)
1 Douglas Aircraft Company, Inc., El Segundo, Calif. (Aerodynamics Section, A. M. O. Smith)
1 Electric Boat Division, General Dynamics Corporation, Groton, Conn.
1 Engineering Societies Library, New York
2 Experimental Towing Tank, Stevens Institute of Technology, Hoboken, N. J.
A. Suarez (1)
Dr. V. Breslin (1)
1 General Electric Company, Missile and Ordnance Systems Department, Pittsfield, Mass. (Engineering Librarian)

1 General Electric Company, Schenectady (Librarian, LMEE Department)
1 Gibbs and Cox, Inc., New York (Dr. S. Hoerner)
1 Grumman Aircraft Engineering Corporation, Dynamics Development Division, Babylon, New York
1 Harvard University, Cambridge, Mass. (Prof. G. Birkhoff, Department of Mathematics)
1 Hudson Laboratories, Columbia University, Dobbs Ferry, N. Y.
2 Hydrodynamics Laboratory, CIT, Pasadena
  Dr. V. A. Vanoni (1)
  T. Kiceniuk (1)
1 Hydronautics, Inc., Rockville, Md.
1 Massachusetts Institute of Technology, Cambridge (Hydrodynamics Laboratory)
1 New York University, Institute of Mathematical Sciences, New York
3 Ordnance Research Laboratory, Pennsylvania State University
  Development Contract Administrator (1)
  Dr. B. W. McCormick (1)
  Dr. G. F. Wislicenus (1)
1 Reed Research, Inc., Washington D. C.
1 Rensselaer Polytechnic Institute, Troy, N. Y. (Department of Mathematics)
1 Scripps Institution of Oceanography, University of California, La Jolla
1 Stanford University, Stanford, Calif. (Applied Mathematics and Statistics Laboratory)
2 State University of Iowa, Iowa Institute of Hydraulic Research, Iowa City
  Prof. H. Rouse (1)
  Prof. L. Landweber (1)
1 Technical Research Group, New York (Dr. J. Kotik)
1 The Rand Corporation, Santa Monica, Calif.
  Dr. Blaine Parkin (1)
  Technical Library (1)
1 The University of Southern California, Los Angeles (Engineering Center, Dr. Raymond Chuan)
1 University of California, Engineering Department, Berkeley (Prof. J. V. Wehausen)
1 University of Maryland, Institute of Fluid Dynamics and Applied Mathematics, College Park
2 University of Michigan, Ann Arbor
  Prof. C. S. Yih, Department of Engineering Mechanics (1)
  Prof. V. Streeter, Department of Civil Engineering (1)
1 University of Minnesota, St. Anthony Falls Hydraulic Laboratory, Minneapolis
1 University of Wisconsin, Mathematics Research Center, Madison (Prof. L. M. Milne Thompson)

1 Webb Institute of Naval Architecture, Glen Cove, N. Y. (Technical Library)
1 Westinghouse Electric Corporation, Baltimore (Engineering Librarian)
1 Westinghouse Research Laboratories, Pittsburgh
1 Woods Hole Oceanographic Institute, Woods Hole, Mass.

NOTS C.L. 1023 3/60 200